UDC 681.883.41

O.V. Onyshchuk postgraduate., S.T. Baras Cand. Sc. (Eng.), Assist. Prof.

GENERALIZED MODEL OF DOPPLER SIGNAL OF THE HYDROACOUSTIC LOG

The mathematical model has been analyzed and the computer physical modeling of Doppler signals has been performed. As a result, the model of the Doppler signal of the hydroacoustic log has been proved and generalized.

Keywords: *echo signal, hydroacoustic log, Doppler shift of frequency, mathematical model, physical model*

Introduction

The Doppler signal structure is to be considered the most essential one among the sources of errors in measuring vector constituents of surface and submarine floating speed of an object by means of a hydroacoustic log [1]. It is the Doppler signal structure that affects the maximum potentialities as to measuring the frequency of high-frequency filling and hereby defines the Doppler log error. Consequently, the detailed study of the Doppler signal is a vital problem of potential accuracy determination in measuring vector constituents of carrier velocity by means of a hydroacoustic log.

Recent Research Analysis

The results of the recent research of the Doppler signals of the hydroacoustic log in the actual floating conditions have been presented in [2]. The analysis of these results allowed the identification of the fine structure of the signals that is the behavioral laws of their high-frequency filling and bypass as well as the connection of the precision of Doppler shifts of frequency measurement with the above stated structure. But the study of actual Doppler signals is ineffective due to their transiency, analysis of their mathematical and physical models therefore being the most reasonable way.

The mathematical model of the Doppler signal has been outlined in [3]; being the result of the conception of the signal on the receiving antenna as a total of a great number of bottom radiated elementary echo-signals (Huygens's principle):

$$s(t)=\sum_{m=1}^{M(t)} A_m \cos\left[\Psi_m(t)\right], \tag{1}$$

where $A_m, \Psi_m(t)$ are assigned to the amplitude and the phase of m elementary echo-signal and *M(t)* – to the number of elementary echo-signals altering by time varying and depending on the receiving moment and the duration of each echo-signal.

Problem Stating

The suggested model [2] cannot be regarded as an illustrative one, thus, in order to make its detailed analysis some extra modifications utilizing the appropriate mathematical apparatus are necessary. This kind of analysis should be directed to detecting the special features of signal structure with a view to ascertain the options of the frequency measuring being as accurate as possible.

Highly convenient for the structure study is a physical model of the Doppler signal that might be obtained as a result of the computer modeling process.

The comparative analysis of the mathematical and physical models of the Doppler signal will therefore firstly - ensure the impartial outcomes and secondly - define the generalized and formalized model of the Doppler signal, the one that will definitely direct towards the substantiated approaches as far as attaining of the maximum measuring accuracy of frequency is concerned. These very problems has this article been dedicated to.

The Analysis of the Mathematical Model

The expression (1) having been analyzed, the structure of the summary signal *s(t)* is obvious to depend upon the parameters of its elementary echo-signals constituents. Every elementary echo-signal is described by its individual amplitude and phase being determined by means of special features of scattering bottom surface, the Doppler effect as well as by means of varying distance every signal is to travel starting from the moment of radiation and terminating in its being received by a log antenna within the angles of direction characteristic curve on account of carrier motion [3]. As this takes place every elementary echo-signal appears as a narrowband process, the summary signal thus can be considered a narrowband one as well. Then, to analyze the fundamental parameters of such signals a well-known Gilbert device can be used [4], according to which the bypass *A (t)* of the summary vibration (1) is determined as a module of the corresponding analytic signal:

$$A(t)=\sqrt{s_m{}^2(t)+\hat{s}_m{}^2(t)}=\sqrt{\left[\sum_{m=1}^{M(t)} A_m \sin\left[\Psi_m(t)\right]\right]^2+\left[\sum_{m=1}^{M(t)} A_m \cos\left[\Psi_m(t)\right]\right]^2}\ , \tag{2}$$

where $\hat{s}(t)$ is a joined expression of *s(t)*.

The complete phase $\Psi(t)$ of the signal $s(t)$ equals to independent variable of the analytical signal:

$$\Psi(t)=arctg\,\frac{\hat{s}(t)}{s(t)}=arctg\,\frac{\sum_{m=1}^{M} A_m \sin\left[\Psi_m(t)\right]}{\sum_{m=1}^{M} A_m \cos\left[\Psi_m(t)\right]}\,. \tag{3}$$

And, finally, the instantaneous frequency $\omega(t)$ of the signal $s(t)$ is a derivative of the complete phase by time varying:

$$\omega(t)=\frac{d}{dt}arctg\,\frac{\hat{s}(t)}{s(t)}=\frac{d}{dt}arctg\,\frac{\sum_{m=1}^{M(t)} A_m \sin\left[\Psi_m(t)\right]}{\sum_{m=1}^{M(t)} A_m \cos\left[\Psi_m(t)\right]}\,. \tag{4}$$

Expressions (2), (3) and (4) are complicated for theoretical calculation of echo-signals $s_{m-1}(t)$ and $s_{m+1}(t)$ being described by the angles of radiation $a+\Delta\gamma$, $a-\Delta\gamma$ and ones of receiving $\beta+\Delta\gamma$, $\beta-\Delta\gamma$ respectively. These angles along with the depth of the local water area determine the amplitudes of these signals A_{m-1}, A_{m+1} as well as the frequency ω_{m-1}, ω_{m+1} [3].

By means of the expression (2) we obtain the bypass of the summary vibration of both elementary echo-signals:

$$A(t)=\sqrt{A_{m-1}{}^2+A_{m+1}{}^2+2A_{m-1}A_{m+1}\cos\left[\Psi_{m+1}(t)-\Psi_{m-1}(t)\right]}\,. \tag{5}$$

The expression (5) corroborates the fact of the summary vibration bypass becoming oscillatory on addition the vibrations with the close values of amplitude and frequency.

The vibration period of the summary vibration bypass is determined by the cosine of the difference between the elementary echo-signals phases.

The phase of the summary vibration of both elementary echo-signals is equal to:

$$\Psi(t,A) = (\omega_0 + \omega_D)t + \Delta\varphi(t) = \omega t + arctg\left\{ \frac{\frac{A_{m-1}}{A_{m+1}} \sin\left[\Psi_{m+1}(t) - \Psi_{m-1}(t)\right]}{1 + \frac{A_{m-1}}{A_{m+1}} \cos\left[\Psi_{m+1}(t) - \Psi_{m-1}(t)\right]} \right\}, \tag{6}$$

with ω_0 representing the filling frequency of the radiated radio pulse, ω_D - the Doppler frequency of the total oscillation and $\Delta\varphi(t)$ - the constituent of the complete phase of the signal under study, the one depending on the phases difference and the amplitudes of the elementary echo-signals ratio.

The instantaneous frequency of the high-frequency signal filling obtained from adding echo-signals is a derivative of the instantaneous phase $\Psi(t,A)$ and as a result of the conversions looks like:

$$\omega(t,A) = \omega_0 + \omega_Д + \Delta\omega \frac{\frac{A_{m-1}^2}{A_{m+1}^2} - 1}{\frac{A_{m-1}^2}{A_{m+1}^2} + 1 + 2\frac{A_{m-1}}{A_{m+1}} \cos\left[\Psi_{m+1}(t) - \Psi_{m-1}(t)\right]}, \tag{7}$$

where $\Delta\omega$ is the half-difference between the frequencies of the elementary echo-signals.

The formula (7) classifies the frequency of the high-frequency filling of the Doppler signal consisting of: the filling frequency of the radiated radio pulse ω_0; the Doppler frequency ω_D being the result of the motion of the floating object and the time-dependent variable $\Delta\omega(t)$ occurring as a result of addition of the elementary echo-signals and is defined be the half-difference between the frequencies and the amplitudes ratio of the elementary echo-signals. It should be mentioned here, that the Doppler signal is determined by the unified elementary echo-signal defined by the angles of radiation α and reception c provided that the width of the log directivity data be infinitely narrow, in so doing the third summand in the formula (7) is lost.

Analyzing the expressions (5) (6) and (7) one can affirm that the signal under study is an oscillation with amplitude and angular alterations. Their principles depend on the ratio of the amplitudes A_{m-1} / A_{m+1} and the phases' difference $\Delta\Psi(t) = \Psi_{m+1}(t) - \Psi_{m-1}(t)$ of the constituents of the elementary echo-signals. Hence, by the instrumentality of the expressions (5) (6) and (7) let's consider the alterations evolution regarding amplitude, phase and instantaneous frequency of the total oscillation subject to the elementary echo-signals amplitudes ratio within an oscillation period of the total signal bypass.

Fig. 1*a, b* and *c* show the spatial graphs where the amplitude, phase and instantaneous frequency of the total oscillation are laid off along the applicate axis respectively, an oscillation period of the total signal bypass is laid off along the *Y*-axis and the elementary echo-signals amplitudes ratio - along the *X*-axis.

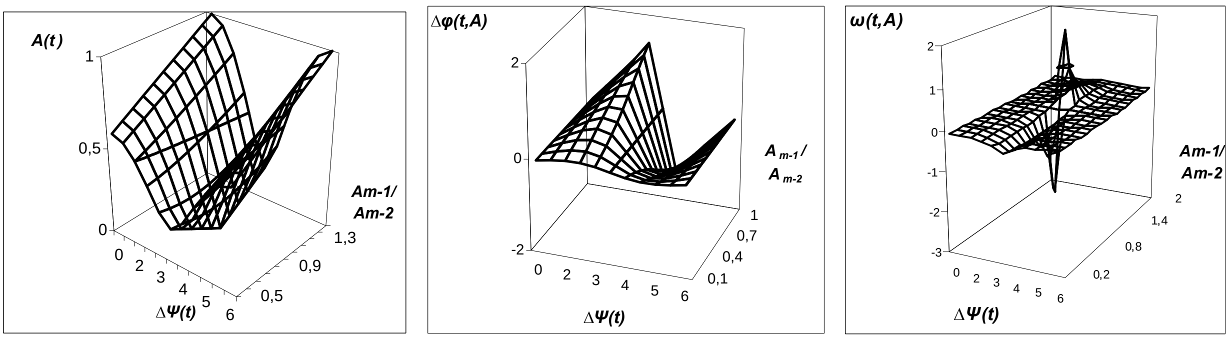

a *b* *c*

Fig.1 - Alterations evolution of the bypass (*a*), the phase (*b*), and the instantaneous frequency (*c*) of the total of two elementary echo-signals

Fig.1 demonstrates that upon adding of 2 elementary echo-signals the total oscillation is defined by the amplitude modulation with a significant depth complexity. Its bypass varies according to the quasiharmonic law and represents the slowly varying time function. Provided the phases' difference of the elementary echo-signals equals *0* or 2π the total oscillation bypass takes on the value of its maximum and if the phases difference is equal to π – the bypass is in its minimum.

The analysis of fig.1*b* demonstrates that the total oscillation phase is a slowly varying time function, the elementary echo-signals amplitudes ratio being lower than 1, but the elementary echo-signals amplitudes ratio approximating 1 and the phases difference being equal to π, the total oscillation phase changes its value rapidly (jump-like), videlicet the phase manipulation takes place. On doing that, the instantaneous frequency being the phase derivative can't be assumed as a slowly varying time function, some positive and negative emissions are observed in its pattern of change, present in the spatial graph (fig.1 *c*).

Consequently, the total oscillation of 2 elementary echo-signals is characterized by the amplitude and angular changes, and possesses phase manipulation and instantaneous frequency emissions.

It should be mentioned that phase manipulation, instantaneous frequency emissions and decreasing of bypass amplitude to its minimum take place simultaneously the phase difference of the elementary echo-signals value approximating or being equal to π. And vice versa, if the phase difference of the elementary echo-signals value doesn't equal π the instantaneous frequency becomes stable, the bypass reaches its maximum and the total oscillation phase varies according to the harmonic law and represents the slowly varying time function.

This statistical connection between the basic parameters of the signal under study is of high practical value for defining conditions as far as the increasing of the precision of Doppler shifts of frequency measurement concerned.

The Computer Simulation and the Doppler Signal Analysis

It should be stated that the total of the two partial echo-signals alone can't reproduce the structure of the studied signal to the full extent taking into consideration the correctness of the approach. As stated above, the theoretical calculation of the oscillation in the form of the total of a number of elementary echo-signals proves to be difficult and laborious. In this context there arises the necessity of attracting modern high-speed data-processing devices for computer generated signal simulation according to the mathematical model (1) in order to further research the Doppler signal in the form of the total of a number of elementary echo-signals.

Since this article discusses the structure of the Doppler signals and the most accurate reproduction of the laws of their bypass variation and the high-frequency filling before simulating the signals according to the model (1) some restrictions should be determined:

the floating object moves evenly and straightforwardly;

the bottom area of radiation is homogeneous and invariable;

tossing and other destabilizing factors are absent;

simulation is limited by the signal emission starting from the moment of radiation and terminating in its being received by a log antenna.

Simulation is performed for different velocities of the carrier, area of water depths and duration of the radiated signal. The above stated computer generated simulation conditions allow identification of the studied signal structure with no influence of distorting and destabilizing factors of the forming, emission and signals data processing environment. Therefore, immediate nature of the Doppler signals: their bypass behaviour and high-frequency filling laws are possible to discuss.

Define the output simulating data. Let radiating and receiving of the radiofrequency pulse be performed according to the first beam of the diametrical-traverse antenna log system its slope relative horizon being $\alpha = 60^0$, and the width of the beam pattern $\gamma = 3^0$. Frequency filling of the radiated signal is $f_0 = 250000 Гц$. Simulation is performed for velocities band *1, 5* and *7 m/s* and widths of *10, 30* and *200m.* The pulse duration is defined according to the recommendations [5]. While simulating some dozens of radiated elements were imitated with them being located within the sonicated bottom area.

The simulation results of the Doppler signals structure are presented in fig.3, fig.4 and fig.*5* introducing instantaneous frequency graphs and the simulated signals spectra respectively. It should be mentioned that, fig. 3*a,* fig.4*a* and fig.5*a* refer to the signal simulated while $V_1 =1m/s$, $H_1=10m$, $\tau_1=10\ ms$. Fig.3*b,* fig.4*b* and fig.5*b* presented for the signal simulated by $V_2=5m/s$, H_2-$30m$, $\tau_2=30ms$, and, finally, fig. 3*c,* fig.4*c* and fig.5*c* define the signal simulated with $V_3=7m/s$, H_3-$150m$, $\tau_3=100ms$. Besides, by comparison, the fig.2*a, b* and *c* show the oscillogram of the actual Doppler signals obtained in the natural floating conditions the velocity of the carrier being *1m/s, 5m/s* and *7m/s*, respectively.

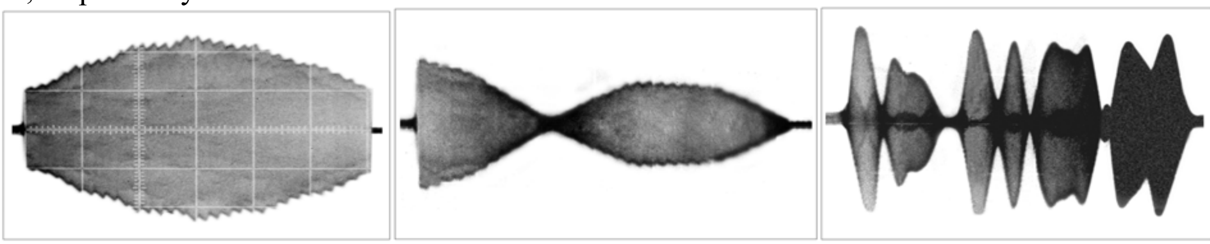

a b c

Fig.2 – Oscillograms of the actual Doppler signals:
a – V_1 =1m/s, b – V_2=5m/s and c – V_3=7m/s

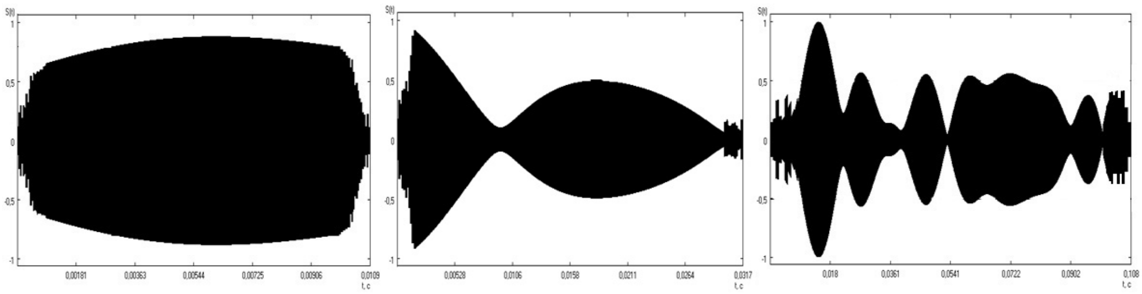

a b c

Fig.3 – Structure of the Doppler signals simulated with:
a – V_1 =1m/s, τ_1=10 ms; b – V_2=5m/s, τ_2=30ms; c – V_3=7m/s, τ_3=100ms

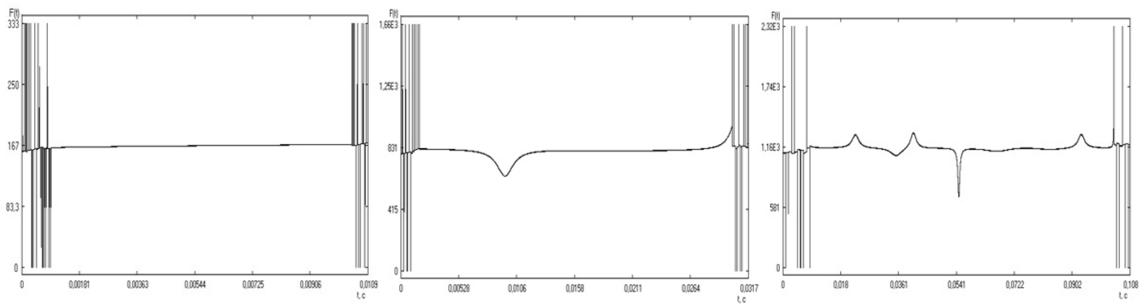

a *b* *c*

Fig.4 – Graphs of the instantaneous frequencies of the Doppler signals simulated with:
a – V_1 =1m/s, τ_1=10 ms; b – V_2=5m/s, τ_2=30ms; c – V_3=7m/s, τ_3=100ms

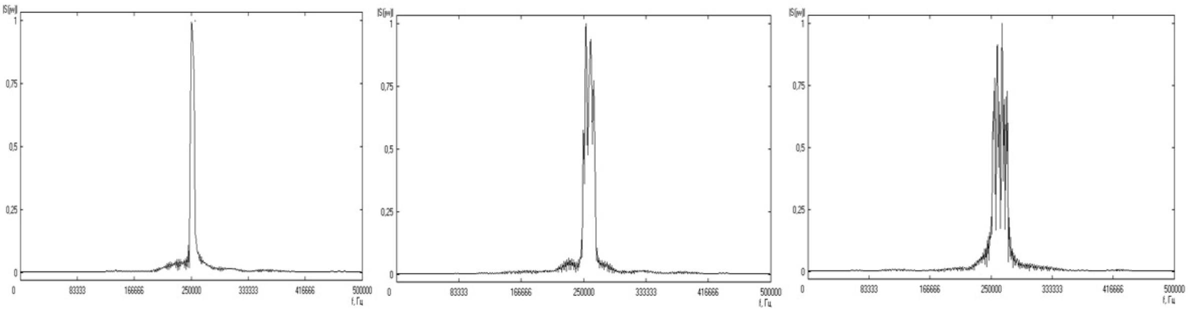

a *b* *c*

Fig.5 – Graphs of the Doppler signals spectra simulated with:

a – V_1 =1m/s, τ_1=10 ms; b – V_2=5m/s, τ_2=30ms; c – V_3=7m/s, τ_3=100ms

The analysis of the structure of the simulated and actual Doppler signals should go first. The form of the simulated signals (fig.3) is similar to the actual Doppler signals (fig.*2*).

Among other factors, when the velocities of the actual (fig.1*a* and *b*) and simulated (fig. 3*a* and *b*) Doppler signals oscillogram are low they resemble the amplitude-simulated oscillations with low-frequency, similar to the harmonic form, bypass.

Velocities being high the Doppler signals oscillogram (fig. 2*b*) demonstrates the increase of the amplitude simulation frequency and a significant divergence with the harmonic law of simulation and assuming the form of the noise-like simulating signal. The similar bypass behaviour is observed in the physical model of the Doppler signal simulated at high velocity (fig.3*c*).

Apart from this, significant high-frequency bypass fluctuations are observed along the front sections of the simulated signals being determined by means of special features of forming and emissing the Doppler signals starting from the moment of radiation and terminating in its being received by a log antenna [3]. These fluctuations are not noticeable in the oscillograms of the actual signals, obviously, this being due to the band-pass filter (“pulling and flattening” of the signals fronts), on the output of which the given oscillograms are obtained (fig.2).

Consider the fine structure of high-frequency filling of the simulated signals. To perform this we make use of the instantaneous frequency graphs (fig.4). These graphs define the frequency value having been determined for every period of high-frequency filling of the simulated signals by means of the formula:

$$F_{Di} = 1/T_i - f_0$$

with f_0 as a filling frequency of the radiated radio-frequency pulse, *i* – as an ordinal number of the period and T_i - as duration of the i-period of the high-frequency filling of the simulated signal.

Consequently, the graph defines the instantaneous values of the Doppler shifts of frequency F_{Di} within the simulated signal (fig.4).

In the first place, it should be mentioned that the extreme right and left frequency sections of all the graphs are defined by significant frequency fluctuations and the central section – by the smooth lines altering relatively slow according to the specific law. This means that the frequency remains relatively stable in the central section of the simulated signal exclusive of the sections where the bypass is in its minimum.

In analyzing the instantaneous frequency graphs (fig.4) and the corresponding bypasses of the simulated signals (fig.3) it should be mentioned that there exist some regularity and interconnection in the behaviour patterns of the bypass and instantaneous frequency of the signals: in the signal sections where the bypass amplitude is in its maximum the corresponding values of the instantaneous frequencies remain invariable on a level with the horizontal line conforming to the Doppler frequency value defined for the central axis of the beam pattern of the log antenna. In the signal sections with the minimal bypass amplitude the instantaneous frequencies shift relative to the Doppler frequency rapidly according to the specific law: they take the form of positive “peaks” or negative “downfalls” the Doppler frequency divergence going on up and down. Thus some number of fragments can be distinguished within the simulated signals being defined by means of the stable as well as unstable Doppler frequency values.

Finally, we proceed to the graphs of the Doppler signals spectra represented in fig.5. On being analyzed they demonstrate that the velocity increase results in the expansion and the shift of the signal spectrum. Herewith a great number of extra spectral peaks emerge making the definition of the accurate Doppler frequency value by means of spectral methods complicated.

Taking into consideration the instantaneous frequency behaviour and the simulated signals bypass as well as the interconnection between them there arises the possibility to divide each signal into three types of fragments and to provide the quantitative analysis of the Doppler frequency within separate fragments. The fragments of the *1st* correspond with the signal sections within which the bypass is in its maximum and the corresponding instantaneous frequencies are stable and invariable (are in the form of horizontal line). The fragments of the 2nd type conform to the sections of the model signal with the minimum bypass and the corresponding instantaneous frequencies rapidly shifting with respect to the Doppler frequency (are in the form of positive “peaks” and negative “downfalls”). And, finally, the fragments of the 3rd type are referred to as the sections of the fore and back fronts of the simulated signals differing from the above stated and being defined by the significant fluctuations of the filling frequency and the amplitude.

Within each fragment we define the arithmetic mean value F_{Dj} together with the root-mean-square deviation σ_{Fj} of the Doppler frequency according to the noted formulae:

$$\bar{F}_{Дj} = \frac{\sum_{i=1}^{n_j} F_{Дi}}{n_j}, \qquad \sigma_{Fj} = \sqrt{\frac{\sum_{i=1}^{n_j} (\bar{F}_{Дj} - F_{Дi})^2}{n_j}},$$

where j- is the ordinal number of the fragment of the proper type, n_j - the number of the periods of the high-frequency filling in the j-fragment.

Subsequently, the calculation results for the similar fragments types were consolidated according to the similar formulae. The final calculation results have been put down into the Table. 1:

Table 1

The Doppler frequency study results in the different fragments of the simulated signals

V, m/s	Fragments of the 1st type			Fragments of the 2nd type			Fragments of the 3rd type (fronts)		
	τ, s	$\Delta F_D, Hz$	σ_F, Hz	τ, s	$\Delta F_D, Hz$	σ_F, Hz	τ, s	$\Delta F_D, Hz$	$\sigma_F, кHz$
1	0,07	3	7	0,002	35	55	0,002	1-15	70-100
5	0,010	2	6	0,010	40	50	0,004	1-10	30-50
7	0,400	4	9	0,400	30	60	0,020	0,2-1	2-10

Analyzing the results submitted in Table 1 we should mention that the duration of the 1st and the 2nd fragments are approximately equal and the fronts duration of the signals under study makes almost 10 percent of the total signal duration. The difference by module between the theoretical value of the Doppler frequency F^*_D (obtained by means of the classical formula $F^*_D = f_0 \frac{2V}{c} \cos\alpha$) and the experimental F_D, as well as the root-mean-square deviation σ_F of the Doppler frequency constitute: for the fragments of the 1st type – units of hertz, for the fragments of the 2nd type – dozens of Hertz and for the fragments of the 3rd type – dozens and hundreds of hertz.

The Generalization of the Model of the Doppler Signal

The detailed analysis of the mathematical model (1) and the corresponding physical model of the Doppler signals reflects, in the first place, the well-known special features of these signals explained in the classical literature and confirmed by the experimental research, namely:

1. The Doppler signal represents the narrowband quasiharmonic random process generally defined by the expression $s(t) = A(t)\cos[\Psi(t)]$ [6].

2. The Doppler signal structure becomes complicated and modified as the carrier velocity increases [7].

3. The Doppler signal spectrum is continuous; moreover, it expands and shifts along the frequencies axis as the carrier velocity increases [8].

4. Extreme right and left sections (fronts) of the Doppler signal are defined by the significant fluctuations of the bypass and high-frequency filling [9].

5. The received signal duration is higher than that of the radiated radio-frequency pulse [8].

Besides, as a result of the analysis of the mathematical and physical models of the Doppler signals some new, unknown before characteristics of the signals have been detected correlating between one another:

1. The structure of the main fragment of the Doppler signal, unlike the structure of the fore and back fronts of this signal, has been entirely formed and is defined by the smooth quasiharmonic law of bypass and instantaneous frequency alternation.

2. The studied signals contain phase manipulation and instantaneous frequency emissions at points where the bypass amplitude is at its minimum.

3. The instantaneous frequency dispersion of the fragments corresponding with the maximum value of the bypass varies on a level with the units of hertz.

4. The filling frequency in the fronts sections of the simulated signals distinguishes from the frequency value by the dozens of kilohertz within the central section of the Doppler signal.

5. The connection between the bypass and the high-frequency filling of these signals makes the definition of the fragments containing the stable and invariable Doppler frequency values possible.

The global analysis of the mathematical and physical models of the Doppler signal allows stating of the concept of the Doppler signal from the point of view of the most effective approaches to its processing (measuring). This very concept is most conveniently defined in the form of graphical dependencies integratably describing the basic signal parameters behaviour and their interconnections (fig.6). Since such graphical dependencies result from the mathematical and physical models they are reasonably considered as the generalized model of the Doppler signals. Such a model may be highly informative to the researcher in order to choose the most effective algorithms and devices of measuring the basic parameters of the Doppler signals.

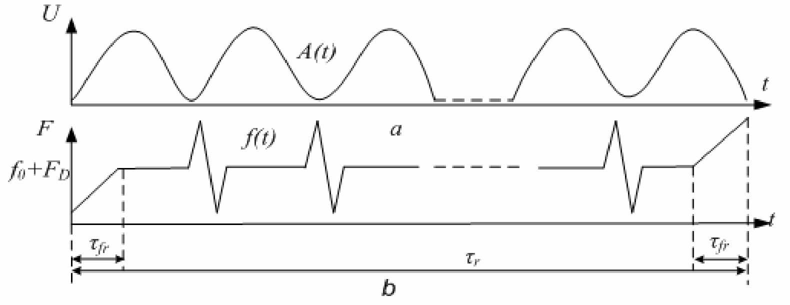

Fig.6- The generalized model of the Doppler signal:
a - the bypass of the signal A(t), b – high-frequency filling f(t).

Conclusions

The given article discusses the basic parameters (bypass, phase and high-frequency filling) of the Doppler signals and the laws of their behaviour by means of the mathematical model (1) and corresponding computer simulation of these signals. The results of the analysis and simulation of the Doppler signals correspond with the present concepts of these signals [6, 8]; their correctness is proven by the experimental research of the actual Doppler signals [7, 9] and reproduce the new special features of these signals. Based on the results obtained the model of the Doppler signal of the acoustic log has been proven and generalized defining the conditions of increase of the measurement accuracy of the Doppler shifts of frequency and, consequently, the carrier motion velocity.

REFERENCES

1. . Барась С. Т. Аналіз джерел похибок вимірювання складових вектора швидкості судна // Вісник ВПІ. – 2000. − № 2. − С. 81 − 85.

2. Барась С. Т. Аналіз результатів експериментальних досліджень флуктуацій частоти доплерівського сигналу гідроакустичного лага в реальних умовах плавання // Вісник ВПІ. – 2003. − № 5. − С. 81 − 85.

3. Онищук О. В., Барась С. Т. Моделювання доплерівського сигналу // Вісник ВПІ. – 2007. − № 5. − С.143−147.

4. Баскаков С. И. Радиотехнические цепи и сигналы. – М.: Высшая школа, 1988. – 448 с.

5. Барась С. Т., Костюк О. А., Лободзінська Р. Ф. Оптимізація часової діаграми роботи гідроакустичного доплерівського лага// МНТЖ ВОТТП. – 2000. № 2. – С. 87 – 91.

6. Абсолютные и относительные лаги / К.А. Виноградов, В.Н. Кошкарев, Б.А.Осюхин, А.А. Хребтов: Справочник. – Л.: Судостроение, 1990. – 264 с.

7. Барась С. Т. Спектр обвідної доплерівського ехо-сигналу, розсіяного морським дном // Вісник ВПІ. – 2000. – № 5. – С. 74 – 76.

8. Гидроакустические навигационные средства / В. И. Бородин, Г. Е. Смирнов, Н. А. Толстяков, Г. В. Яковлев. – Л.: Судостроение, 1983. – 262 с.

9. Измеритель частоты гидроакустического доплеровского лага А.с. №1700492. СССР. / С. Т. Барась, В. А. Мельник, А. П. Мартынюк – № 4699484/21; Заявлено 31.05.89; Опубл. 23.12.91, Бюл. № 47. – 5с.: ил.

Onyshchuk Oleh Volodymyrovych – Postgraduate of the Department of Computer and Telecommunication Equipment Design;

Baras Svjatoslav Tadionovych – Associate Professor of the Department of Computer and Telecommunication Equipment Design.

Vinnytsya National Technical University